

Supporting Information
for

Improving the mesomorphism in bispyrazolate Pd(II) metallocmesogens: An efficient platform for ionic conduction

Cristián Cuerva,^{*a} Mercedes Cano^a and Rainer Schmidt ^{*b}

^a MatMoPol Group. Department of Inorganic Chemistry, Faculty of Chemical Sciences, Complutense University of Madrid, Ciudad Universitaria, E-28040 Madrid, Spain. E-mail: c.cuerva@ucm.es.

^b GFMC. Departamento de Física de Materiales, Universidad Complutense de Madrid, Ciudad Universitaria, E-28040 Madrid, Spain. E-mail: rainer.schmidt@fis.ucm.es.

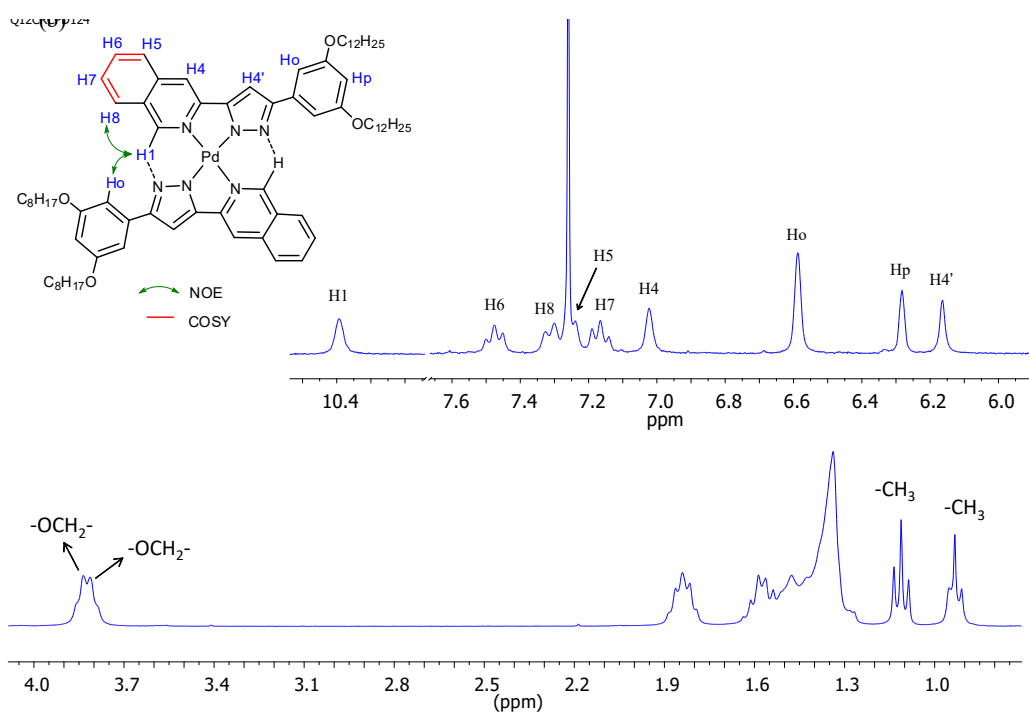


Figure S1. (a) Partial ^1H -NMR spectrum of $[\text{Pd}(\text{pz}^{\text{R}(12,12)\text{iq}})(\text{pz}^{\text{R}(8,8)\text{iq}})]$ **3** showing the aromatic region. The NOE effects and COSY correlations are indicated. (b) Partial ^1H -NMR spectrum of $[\text{Pd}(\text{pz}^{\text{R}(12,12)\text{iq}})(\text{pz}^{\text{R}(4,4)\text{iq}})]$ **1** showing the aliphatic region.

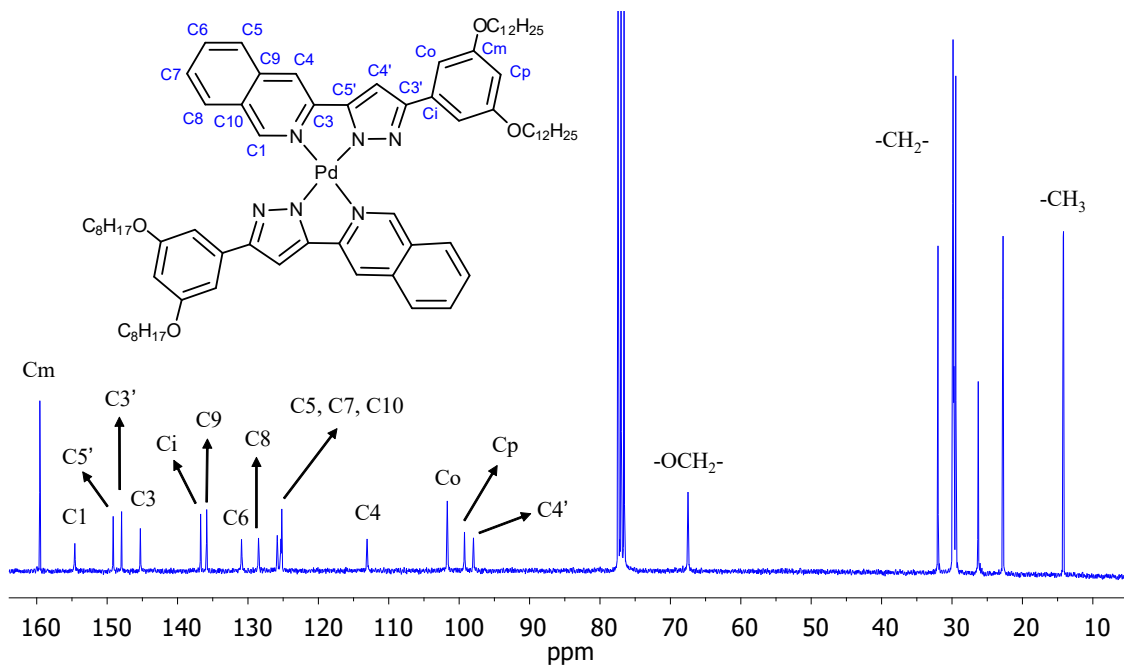


Figure S2. ^{13}C -NMR spectra of $[\text{Pd}(\text{pz}^{\text{R}(12,12)\text{iq}})(\text{pz}^{\text{R}(8,8)\text{iq}})]$ **3**, recorded in CDCl_3 solution at 298 K.

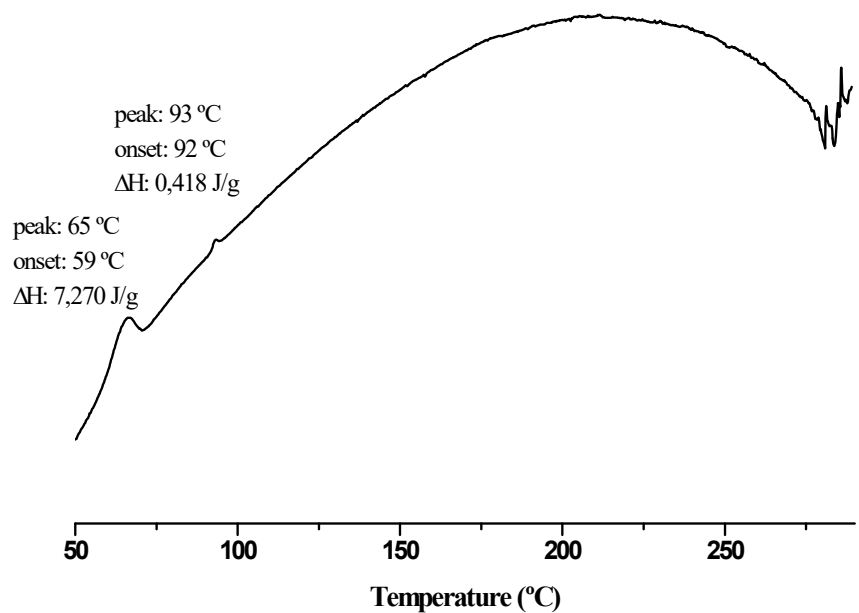


Figure S3. DSC thermogram recorded for the compound $[\text{Pd}(\text{pz}^{\text{R}(12,12)\text{iq}})(\text{pz}^{\text{R}(4,4)\text{iq}})]$ **1** during the first heating cycle.

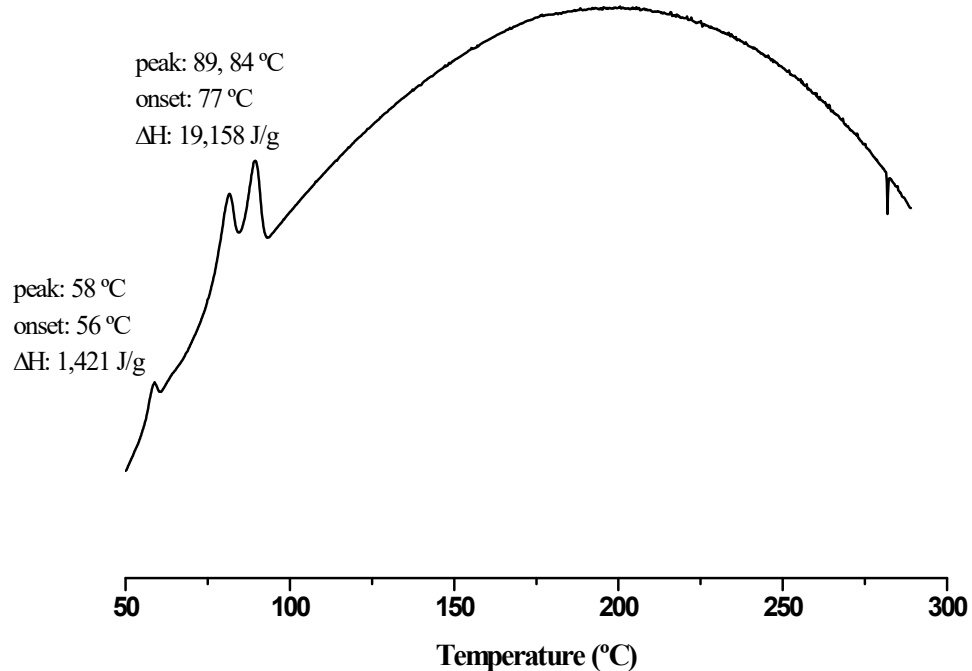


Figure S4. DSC thermogram recorded for the compound $[\text{Pd}(\text{pz}^{\text{R}(12,12)\text{iq}})(\text{pz}^{\text{R}(6,6)\text{iq}})]$ **2** during the first heating cycle.

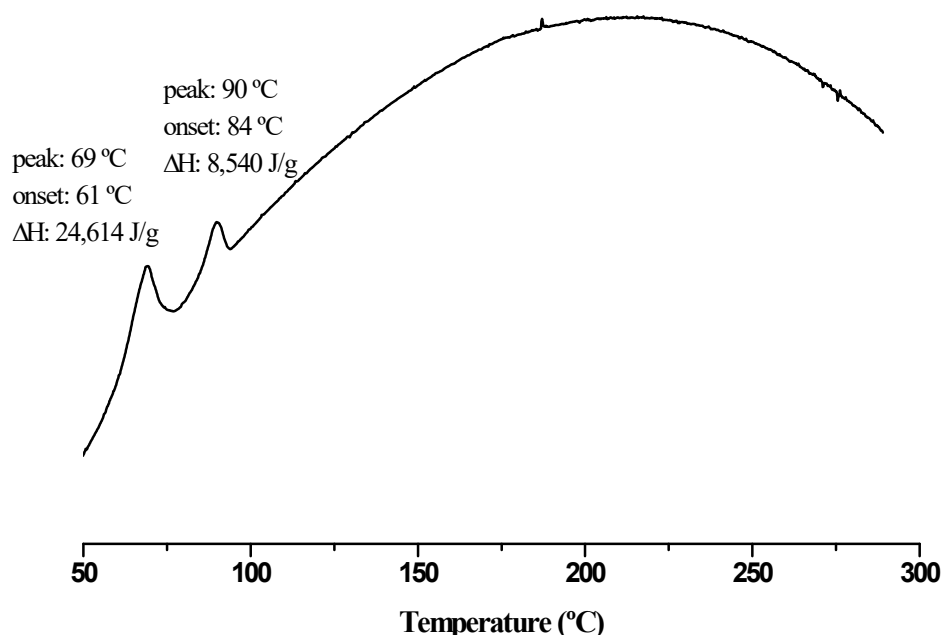


Figure S5. DSC thermogram recorded for the compound $[\text{Pd}(\text{pz}^{\text{R}(12,12)\text{iq}})(\text{pz}^{\text{R}(8,8)\text{iq}})]$ 3 during the first heating cycle.

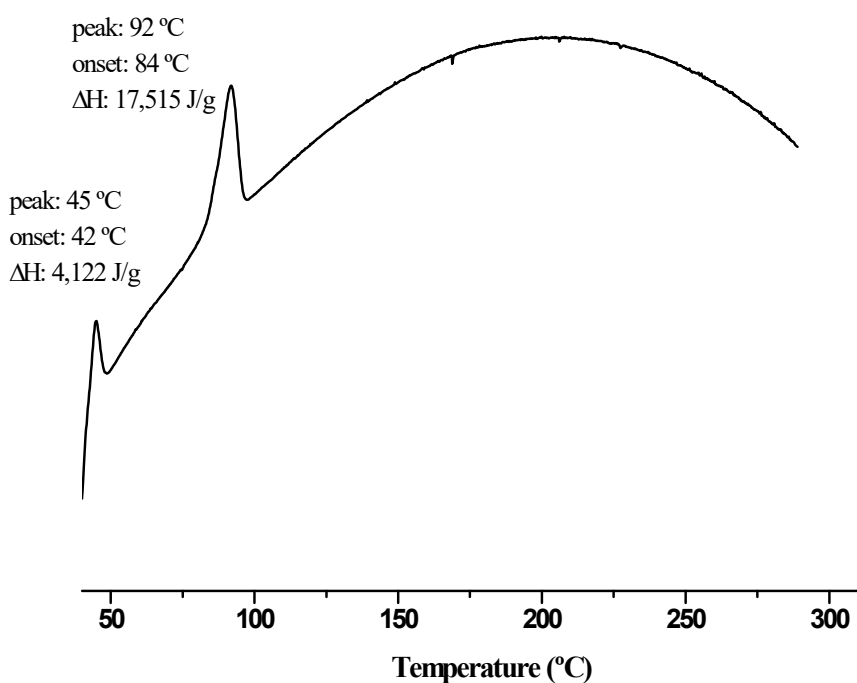


Figure S6. DSC thermogram recorded for the compound $[\text{Pd}(\text{pz}^{\text{R}(12,12)\text{iq}})(\text{pz}^{\text{R}(10,10)\text{iq}})]$ 4 during the first heating cycle.

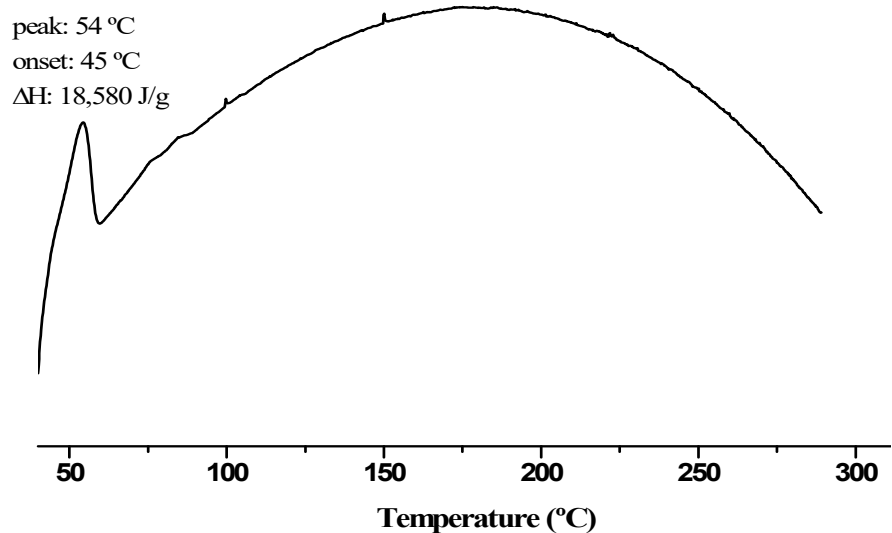


Figure S7. DSC thermogram recorded for the compound $[\text{Pd}(\text{pz}^{\text{R}(12,12)\text{iq}})(\text{pz}^{\text{R}(14,14)\text{iq}})]$ **5** during the first heating cycle.

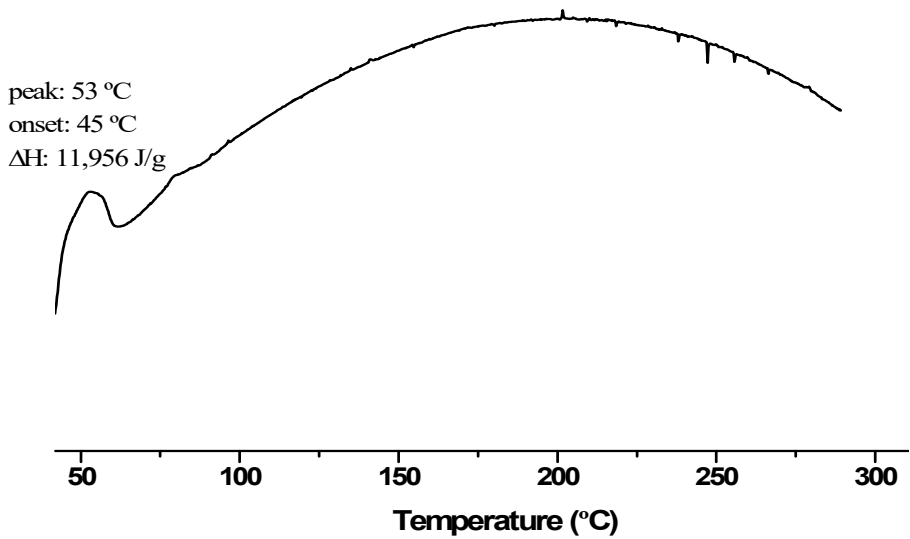


Figure S8. DSC thermogram recorded for the compound $[\text{Pd}(\text{pz}^{\text{R}(12,12)\text{iq}})(\text{pz}^{\text{R}(16,16)\text{iq}})]$ **6** during the first heating cycle.

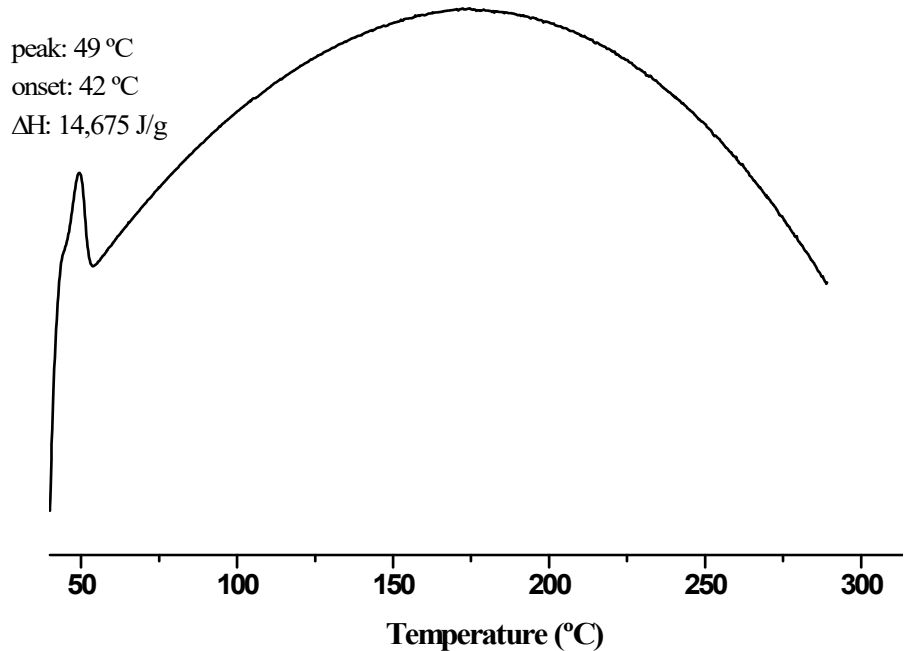


Figure S9. DSC thermogram recorded for the compound $[Pd(pz^{R(12,12)iq})(pz^{R(18,18)iq})] \text{ 7}$ during the first heating cycle.

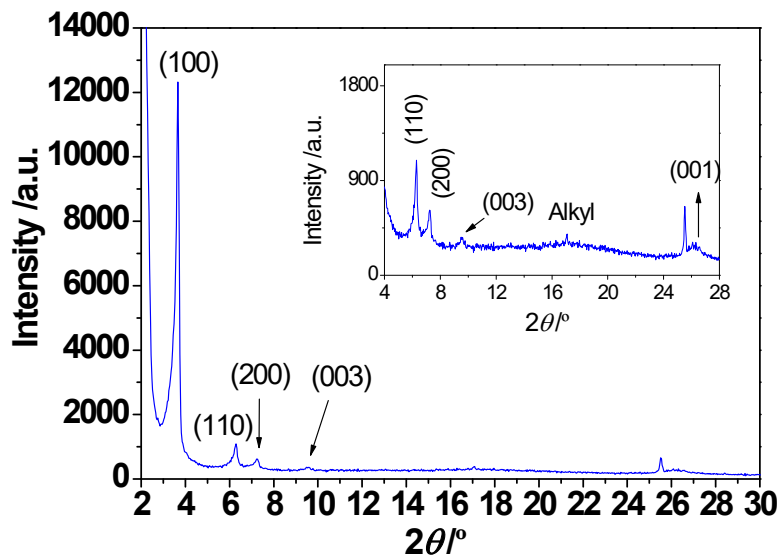


Figure S10. XRD diffractogram for compound $[Pd(pz^{R(12,12)iq})(pz^{R(14,14)iq})] \text{ 5}$ recorded in the Col_h mesophase at 150 °C upon heating.

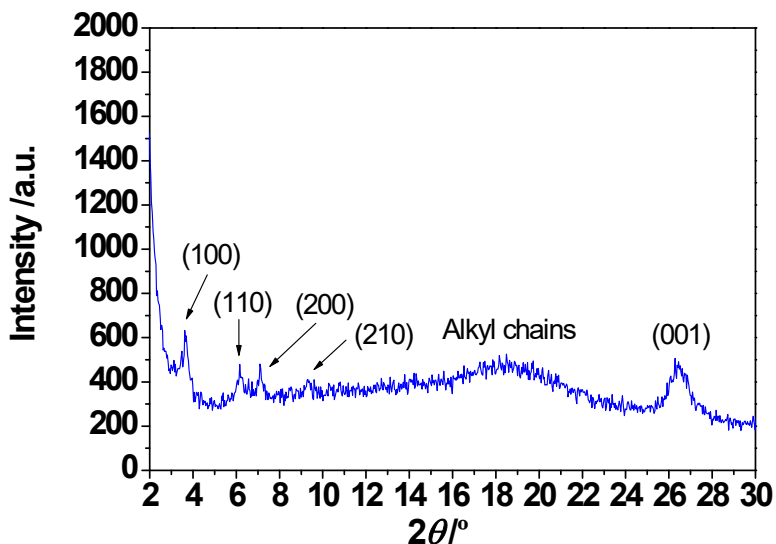


Figure S11. XRD diffractogram for compound $[Pd(pz^{R(12,12)iq})(pz^{R(16,16)iq})]$ **6** recorded in the Col_h mesophase at $80\text{ }^\circ\text{C}$ upon heating.

Table S1. Maximum conductivity values reached in the Col_h mesophase of bispyrazolate-based Pd(II) metallomesogens.

Compound (n)	$\sigma'_{\max} / (\Omega \text{ cm})^{-1}$
[Pd(pz^{R(n,n)py})₂]	
(4)	9.79×10^{-9}
(12)	7.46×10^{-7}
(16)	4.99×10^{-10}
[Pd(pz^{R(n,n)iq})₂]	
(4)	9.93×10^{-9}
(12)	1.34×10^{-6}
(16)	5.95×10^{-7}
[Pd(pz^{R(12,12)iq})(pz^{R(n,n)iq})]	
(6)	6.36×10^{-9}
(10)	6.35×10^{-8}
(14)	4.36×10^{-9}
(18)	4.53×10^{-7}